Functional redundancy between repair factor XLF and damage response mediator 53BP1 in V(D)J recombination and DNA repair

Valentyn Oksenych[a,1], Frederick W. Alt[a,2], Vipul Kumar[a], Bjoern Schwer[a], Duane R. Wesemann[a,b], Erica Hansen[a], Harin Patel[a], Arthur Su[a], and Chunguang Guo[a,1,2]

[a]Department of Genetics, Harvard Medical School, Children's Hospital, Immune Disease Institute, Howard Hughes Medical Institute, Boston, MA 02115; and [b]Division of Rheumatology, Immunology, and Allergy, Department of Medicine, Brigham and Women's Hospital, Boston, MA 02115

Contributed by Frederick W. Alt, December 28, 2011 (sent for review December 12, 2011)

The classical nonhomologous DNA end-joining (C-NHEJ) double-strand break (DSB) repair pathway in mammalian cells maintains genome stability and is required for V(D)J recombination and lymphocyte development. Mutations in the XLF C-NHEJ factor or ataxia telangiectasia-mutated (ATM) DSB response protein cause radiosensitivity and immunodeficiency in humans. Although potential roles for XLF in C-NHEJ are unknown, ATM activates a general DSB response by phosphorylating substrates, including histone H2AX and 53BP1, which are assembled into chromatin complexes around DSBs. In mice, C-NHEJ, V(D)J recombination, and lymphocyte development are, at most, modestly impaired in the absence of XLF or ATM, but are severely impaired in the absence of both. Redundant functions of XLF and ATM depend on ATM kinase activity; correspondingly, combined XLF and H2AX deficiency severely impairs V(D)J recombination, even though H2AX deficiency alone has little impact on this process. These and other findings suggest that XLF may provide functions that overlap more broadly with assembled DSB response factors on chromatin. As one test of this notion, we generated mice and cells with a combined deficiency for XLF and 53BP1. In this context, 53BP1 deficiency, although leading to genome instability, has only modest effects on V(D)J recombination or lymphocyte development. Strikingly, we find that combined XLF/53BP1 deficiency in mice severely impairs C-NHEJ, V(D)J recombination, and lymphocyte development while also leading to general genomic instability and growth defects. We conclude that XLF is functionally redundant with multiple members of the ATM-dependent DNA damage response in facilitating C-NHEJ and discuss implications of our findings for potential functions of these factors.

ataxia telangiectasia-mutated | double-strand DNA break repair | NHEJ1 | Cernunnos

In mammalian cells, double-strand break (DSBs) can be generated extrinsically by ionizing radiation (IR) or by general physiologic factors such as oxidative stress, DNA replication, or transcription. Programmed DSBs are introduced into antigen receptor loci during V(D)J recombination in developing lymphocytes and during Ig heavy chain (IgH) class switch recombination (CSR) in activated mature B lymphocytes. There are two major DSB repair pathways in mammalian cells (1, 2). Homologous recombination (HR) accurately repairs DSBs in the S and G2 phases of the cell cycle; classical nonhomologous DNA end-joining (C-NHEJ) fuses broken DNA ends that lack or have limited homology throughout the cell cycle but predominantly in G1. There are multiple well-characterized C-NHEJ factors (2). The Ku70/Ku80 (Ku) complex recognizes DSBs, and the XRCC4/DNA Ligase IV (Lig4) complex ligates DSBs. DNA-dependent protein kinase, catalytic subunit (DNA-PKcs) is activated by Ku at DSBs and, among other functions, activates Artemis, which processes DSBs. The precise role for the XLF (also called NHEJ1 or Cernunnos) C-NHEJ factor remains unknown; however, XLF recently was found to be functionally redundant with the ataxia telangiectasia-mutated (ATM) protein kinase for C-NHEJ during V(D)J recombination (3).

V(D)J recombination assembles Ig and T-cell receptor variable-region exons from variable (V), diversity (D), and joining (J) gene segments (4, 5). During V(D)J recombination, which occurs in G1, RAG1/2 endonuclease generates DSBs specifically between two V, D, or J segments and adjacent recombination signal sequences (RSs). RAG cleavage generates two hairpin-sealed coding ends (CEs) and two blunt RS ends (SEs). Subsequently, CEs are processed and joined to form coding joins (CJs) and the SEs are joined to form signal joins (SJs). The RAG2 protein restricts V(D)J joining exclusively to C-NHEJ (6, 7). Thus, deficiency for any C-NHEJ factor, except XLF (see below), abrogates V(D)J recombination and blocks B- and T-cell development at the progenitor stage, causing severe combined immune deficiency (SCID) (4, 5). In mature B cells, a second type of Ig gene rearrangement involving DSBs occurs during CSR, allowing different IgH constant-region exons and encoded antibody classes and effector functions to be expressed. For CSR, the activation-induced cytidine deaminase (AID) initiates the introduction of DSBs into long-switch (S) regions that flank constant-region exons. DSB joining during CSR also appears to predominantly use C-NHEJ, but can also be carried out by a still poorly understood alternative end-joining pathway (A-EJ) (8).

ATM is a phosphatidylinositol 3-kinase-like kinase and a key DNA damage sensor. When DSBs occur, ATM autophosphorylates and also phosphorylates numerous DSB response substrates, including histone H2AX and 53BP1. ATM and its substrates have activities in cellular DSB checkpoints and are also involved in DSB repair (4). H2AX is phosphorylated by ATM in nucleosomes surrounding DSBs where it becomes a platform for assembly of ATM-dependent DSB response factors over large chromatin regions. Recruitment of 53BP1 to DSBs does not require H2AX, but H2AX phosphorylation augments 53BP1 accumulation (9). ATM-dependent DSB response foci may tether DSBs and, thereby, enhance efficient repair via C-NHEJ (10). However, deficiency for ATM or 53BP1 causes only modest V(D)J recombination or lymphocyte developmental defects (10, 11); whereas H2AX deficiency alone leads to no obvious defects in these processes (12). Deficiency for DSB response factors also leads to general genomic instability and impairs CSR to significant, but varying, degrees. 53BP1 deficiency impairs CSR far more severely than ATM or H2AX deficiency, suggesting additional roles for 53BP1 in CSR (11, 13). Defective CSR in 53BP1-deficient cells is associated with increased joining of AID-initiated DSBs within S regions and with decreased joining of AID-initiated DSBs between S regions (14), similar to the CSR defects observed in the context of C-NHEJ deficiency (15). On this

Author contributions: V.O., F.W.A., and C.G. designed research; V.O., V.K., D.R.W., E.H., H.P., A.S., and C.G. performed research; V.O., B.S., and C.G. contributed new reagents/analytic tools; V.O., F.W.A., V.K., and C.G. analyzed data; and V.O., F.W.A., and C.G. wrote the paper.

The authors declare no conflict of interest.

Freely available online through the PNAS open access option.

[1]V.O. and C.G. contributed equally to this article.

[2]To whom correspondence may be addressed. E-mail: alt@enders.tch.harvard.edu or cguo@idi.harvard.edu.

basis, 53BP1 has been suggested to enhance longer-range inter-S joining (i.e., CSR) and/or promote S-region DSB joining into C-NHEJ versus A-EJ, thereby favoring intra-S region joining versus inter-S region joining due to the repetitive nature of individual S regions. In accord with such proposals, 53BP1 has been implicated in promoting DNA end mobility and long-range joining in other contexts (16), and it has also been implicated in repair pathway choice by protecting DSBs from ATM-dependent DSB resection during HR and CSR (17, 18).

Like XLF-deficient human fibroblasts, XLF-deficient mouse embryonic stem cells and fibroblasts are IR sensitive and defective for V(D)J recombination on episomal substrates (19). However, XLF-deficient mice have relatively unimpaired lymphocyte development, and XLF-deficient pro–B-cell lines carry out chromosomal V(D)J recombination similarly to WT progenitor (pro)-B lines (20). In this context, subsequent studies revealed ATM and H2AX to be functionally redundant with XLF, as combined XLF/ATM deficiency led to a SCID phenotype associated with a nearly complete loss of ability to undergo C-NHEJ in the context of chromosomal V(D)J recombination (3). Combined XLF and ATM deficiency also impaired C-NHEJ, but not A-EJ, during CSR, indicating redundancy between these two factors in C-NHEJ beyond V(D)J recombination (3). With respect to ATM, this functional redundancy depends on kinase activity and preferentially affects chromosomal versus extrachromosomal V(D)J substrates, suggesting a role for chromatin-bound ATM substrates. Correspondingly, XLF/H2AX double-deficient pro-B lines were also impaired for C-NHEJ during V(D)J recombination that was accompanied by marked resection of RAG-initiated DSBs, consistent with a role for H2AX in protecting such ends from resection (21). On the other hand, such resection was not observed in ATM/XLF-deficient pro-B lines, likely due to the additional role of ATM in activating CtIP endonuclease resection of V(D)J ends. Notably, XLF/H2AX deficiency leads to embryonic lethality in mice, suggesting potential overlapping XLF and H2AX functions in processes beyond those involving ATM (3).

To further test the notion that XLF may provide C-NHEJ functions that overlap with or compensate for those provided by the assembly of ATM-mediated DSB response complexes in C-NHEJ, we tested for functional overlap between XLF and 53BP1.

Results

Combined Deficiency of XLF and 53BP1 Leads to Defects in Lymphocyte Development. Mice doubly deficient for XLF and 53BP1 ($XLF^{\Delta/\Delta}$ $53BP1^{-/-}$) were generated by breeding mice with homozygous deficiency for 53BP1 and heterozygous deficiency for XLF ($XLF^{+/\Delta}$ $53BP1^{-/-}$). In contrast to the embryonic lethality of $XLF^{\Delta/\Delta}H2AX^{-/-}$ mice, $XLF^{\Delta/\Delta}53BP1^{-/-}$ mice were born at a Mendelian ratio although they were significantly smaller than wild-type mice or mice deficient for either XLF or 53BP1 alone (Fig. 1*B*). Total thymocyte numbers in $XLF^{\Delta/\Delta}$ and $53BP1^{-/-}$ mice are modestly reduced (approximately twofold), but otherwise thymocyte development appears relatively normal on the basis of surface CD4 and CD8 differentiation marker staining (22) (Fig. 2). In contrast, $XLF^{\Delta/\Delta}$ $53BP1^{-/-}$ mice had a greater than 30-fold decrease in thymocyte numbers compared with either $XLF^{\Delta/\Delta}$ or $53BP1^{-/-}$ mice (Fig. 1*C*).

A

	XLF+/+53BP1-/-	XLF+/Δ53BP1-/-	XLFΔ/Δ53BP1-/-	Total
Birth	27	47	22	96
Birth (exp)	24	48	24	96

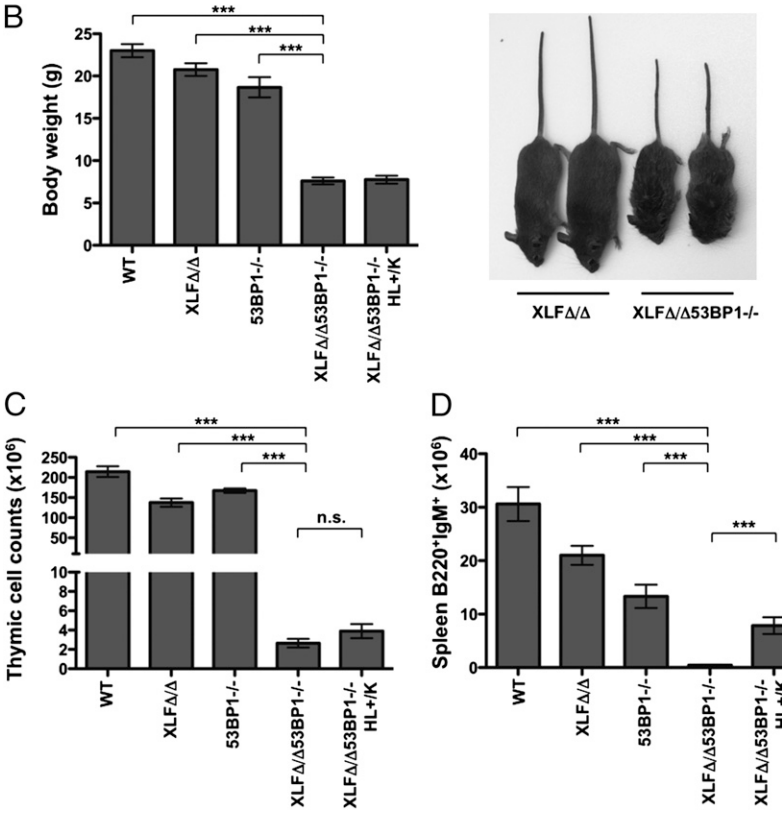

Fig. 1. 53BP1 and XLF have redundant functions in lymphocyte development. (*A*) The number of live-born mice obtained from crosses between $XLF^{+/\Delta}53BP1^{-/-}$ mice. (*B*, *Left*) The total body weight (in grams) of adult mice (4–5 wk old) from the different genotypes as indicated. The data represent the average and the SD from at least three mice of each genotype of each sex. (*Right*) $XLF^{\Delta/\Delta}$ and $XLF^{\Delta/\Delta}53BP1^{-/-}$ mice at 4 wk old. (*C* and *D*) Total thymocyte numbers (*C*) and $B220^{+}IgM^{+}$ splenic B-cell numbers (*D*). Each value listed represents the average ± SD from at least three mice between 4 and 6 wk of age.

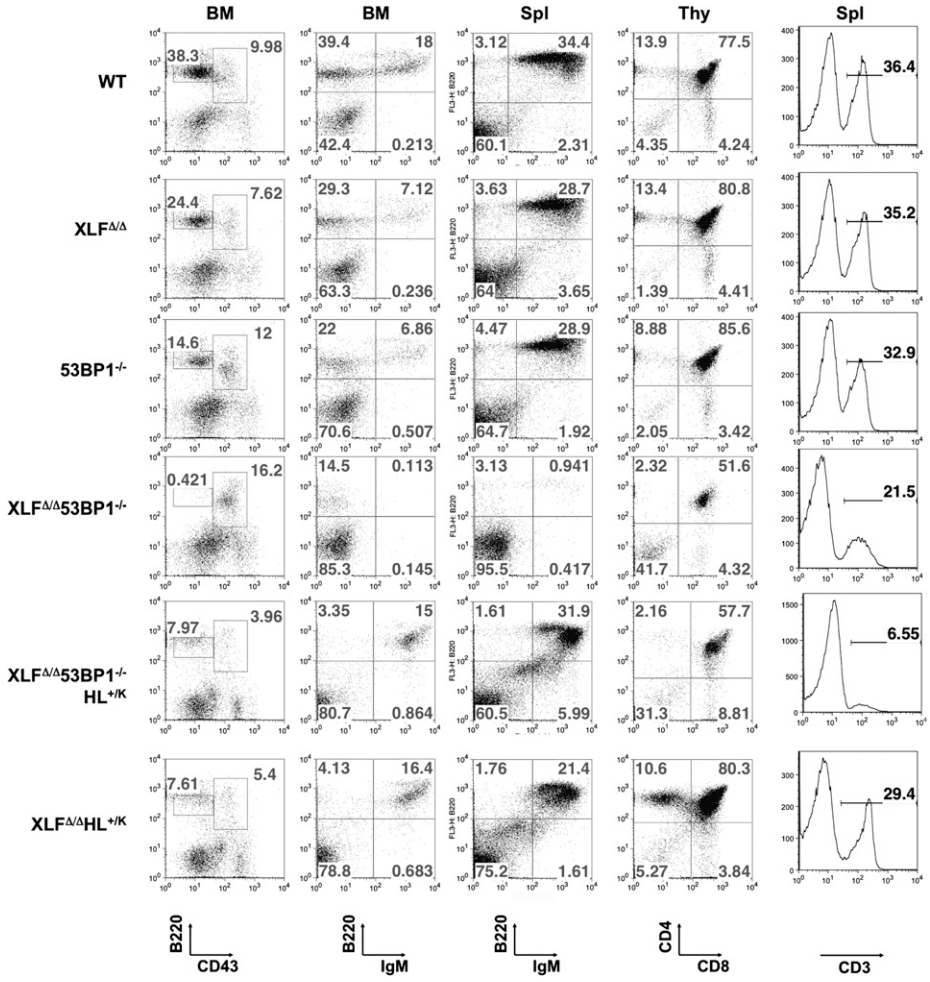

Fig. 2. B- and T-cell development in WT and mutant mice. Representative flow cytometric analyses of bone marrow (BM), spleen (Spl), and thymus (Thy) from wild-type (WT), XLF$^{\Delta/\Delta}$, 53BP1$^{-/-}$, XLF$^{\Delta/\Delta}$53BP1$^{-/-}$, XLF$^{\Delta/\Delta}$ HL$^{+/K}$, and XLF$^{\Delta/\Delta}$53BP1$^{-/-}$HL$^{+/K}$ mice. Numbers on the plot are percentages of total cells represented by the indicated population.

Similar to that of XLF$^{\Delta/\Delta}$ATM$^{-/-}$ mice or other C-NHEJ–deficient mice (3), thymocyte development in XLF$^{\Delta/\Delta}$53BP1$^{-/-}$ mice was impaired at the CD4, CD8 double-negative progenitor stage (Fig. 2). Whereas XLF$^{\Delta/\Delta}$ and 53BP1$^{-/-}$ mice have relatively unimpaired B-cell development with only modestly reduced B220^{+}IgM^{+} splenic B-cell numbers (11, 20), (Figs. 1*D* and 2), XLF$^{\Delta/\Delta}$53BP1$^{-/-}$ mice had few splenic B cells (Fig. 1*D*) with developmental impairment at the CD43^{+}B220^{+} pro–B-cell stage (Fig. 2).

The B- and T-cell developmental defects in XLF$^{\Delta/\Delta}$53BP1$^{-/-}$ mice are consistent with a defect in V(D)J recombination. To further test this possibility, we generated XLF$^{\Delta/\Delta}$53BP1$^{-/-}$ mice that contained *IgH* and *IgL* genes with preassembled variable region exons (referred to as "HL" XLF$^{\Delta/\Delta}$53BP1$^{-/-}$ mice) into the XLF$^{\Delta/\Delta}$53BP1$^{-/-}$ background by breeding. The preassembled IgH and Ig light chain (IgL) knock-in variable region exons bypass the need for Ig variable region assembly to promote B-cell development. These preassembled IgH and IgL loci substantially rescued B-cell, but not T-cell, development in XLF$^{\Delta/\Delta}$53BP1$^{-/-}$ mice (Figs. 1 *C* and *D* and 2). These findings strongly suggest that XLF/53BP1 double deficiency severely impairs lymphocyte development, leading to a SCID phenotype by impairing V(D)J recombination.

XLF and 53BP1 Have Redundant Functions in V(D)J Recombination. To test unequivocally whether XLF$^{\Delta/\Delta}$53BP1$^{-/-}$ pro-B cells have a V(D)J recombination defect, we generated *v-abl*–transformed pro–B-cell lines from WT, XLF$^{\Delta/\Delta}$, 53BP1$^{-/-}$, and XLF$^{\Delta/\Delta}$53BP1$^{-/-}$ mice that carried bcl-2 transgenes. Upon treatment with a v-abl kinase inhibitor (STI571), such *v-abl*–transformed pro–B-cell lines arrest in G1 phase of the cell cycle and activate RAG gene expression, whereas ectopic bcl-2 expression prevents apoptosis associated with v-abl inhibition. In such lines, V(D)J recombination can be assayed via chromosomally integrated V(D)J recombination reporter constructs using a Southern blotting approach. In such assays, the deletional coding join construct, DEL-CJ (10), reveals both CJs and unjoined CEs, whereas the deletional RS join construct, DEL-SJ (10), reveals SJs and unjoined RS ends (SEs). Three separate XLF$^{\Delta/\Delta}$53BP1$^{-/-}$ pro-B lines were assayed after 2 and 4 d of STI571 treatment along with WT, XLF$^{\Delta/\Delta}$, and 53BP1$^{-/-}$ lines. In contrast to the other lines, the XLF$^{\Delta/\Delta}$53BP1$^{-/-}$ pro-B lines showed a severe V(D)J recombination defect as evidenced by substantially reduced recombination products for both CJs and SJs (Fig. 3). In addition, although CJs and SJs were reduced, clear bands corresponding to unjoined CEs or SEs were not observed. The latter phenotype is distinct from that of XLF$^{\Delta/\Delta}$ATM$^{-/-}$ lines, which show a nearly complete loss of CJs and SJs and accumulation of distinct CEs and SEs, but quite similar to that observed with XLF$^{\Delta/\Delta}$H2AX$^{-/-}$ pro-B lines (3). Overall, these results, along with HL rescue results of lymphocyte development, indicate that the SCID phenotype of XLF$^{\Delta/\Delta}$53BP1$^{-/-}$ mice results, at least in large part, from a severe impairment of C-NHEJ during V(D)J recombination.

The absence of obvious accumulation of CEs or SEs in XLF$^{\Delta/\Delta}$H2AX$^{-/-}$ pro-B lines suggests aberrant resection of these ends (3). Such resection appeared similar to the ATM-dependent resection of nonjoined ends in the absence of an end-protective function of ATM-phosphorylated H2AX (γ-H2AX) (21). In this regard, 53BP1 has also been implicated in protecting DSBs from ATM-dependent end resection (17). To test for a potential role for 53BP1 in protecting ends from ATM-dependent resection in XLF$^{\Delta/\Delta}$53BP1$^{-/-}$ pro-B lines, we treated the lines with an ATM kinase inhibitor at

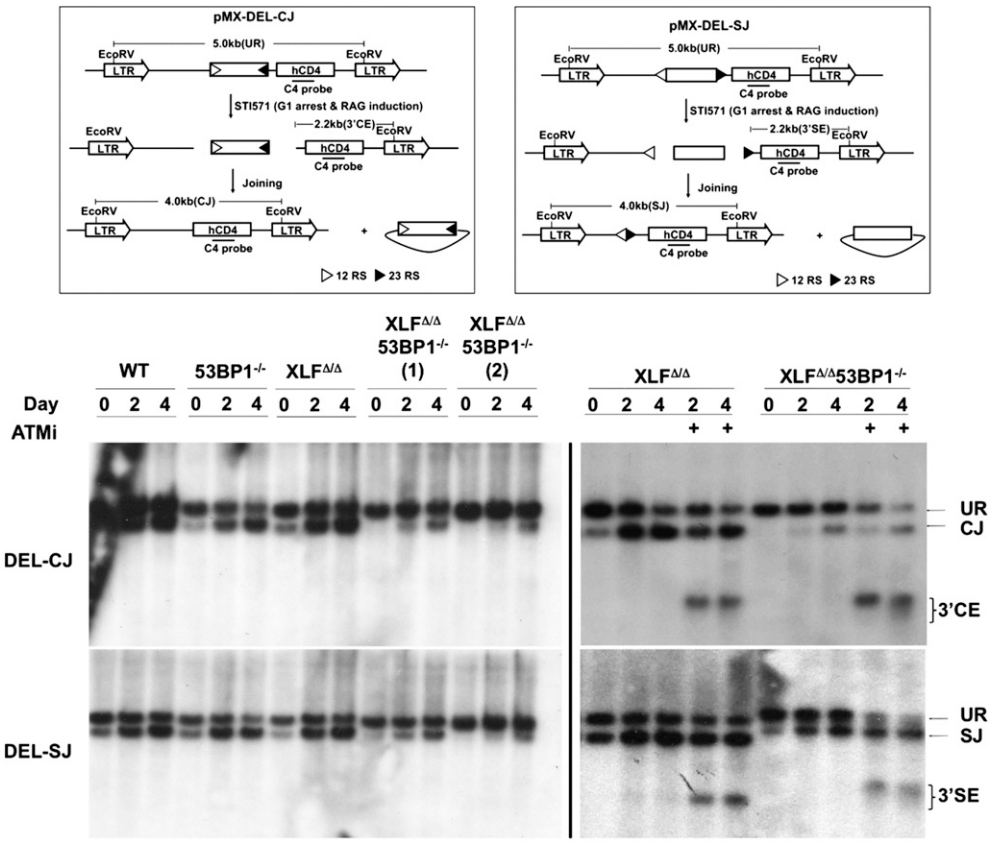

Fig. 3. 53BP1 and XLF have redundant functions in chromosomal V(D)J recombination. (*Upper* panels) Diagram of integrated chromosomal substrates, pMX-DEL-CJ (*Left*) and pMX-DEL-SJ (*Right*). (*Lower* panels) Southern blotting with C4 probe of EcoRV-digested DNA from STI571-treated (2 or 4 d) v-abl pro-B lines containing pMX-DEL-CJ or pMX-DEL-SJ substrates, either with or without ATM inhibitor treatment. Results were obtained from cell pools with diverse substrate integrations. Bands reflecting pMX-DEL-CJ unrearranged substrates (UR), coding ends (3′CE), coding joins (CJ), signal ends (3′SE), and signal joins (SJ) are indicated. WT, wild type.

the same time at which we tested them for V(D)J recombination on integrated substrates. As expected (3), treatment of the $XLF^{\Delta/\Delta}$ lines with the ATM inhibitor (Ku-55933) led to severely reduced CJs and the accumulation of unjoined CEs. Notably, $XLF^{\Delta/\Delta}$ $53BP1^{-/-}$ pro-B lines treated with the inhibitor, although continuing to have severely reduced levels of CEs and SEs, generated unjoined CEs or SEs along with smear below the CE and SE bands that was consistent with aberrant end resection (Fig. 3). These findings were again very similar to what we observed previously by ATM inhibitor treatment of $H2AX^{-/-}XLF^{\Delta/\Delta}$ lines. These findings further suggest that during V(D)J recombination in XLF-deficient cells, 53BP1 functions, beyond any other roles in joining, to protect unjoined CEs and SEs from aberrant resection.

XLF and 53BP1 Have Overlapping Roles in Maintaining General Genomic Stability. To determine whether the potential functional redundancy between XLF and 53BP1 extends to processes beyond V(D)J recombination, we used a telomere-FISH to assay for various types of chromosomal aberrations (mainly chromosome or chromatid breaks) in tail fibroblasts from WT, $Ku70^{-/-}$, $XLF^{\Delta/\Delta}$, $53BP1^{-/-}$, and $XLF^{\Delta/\Delta}53BP1^{-/-}$ mice. Overall, we analyzed fibroblasts from eight WT (466 total metaphases), three $Ku70^{-/-}$ (297 metaphases), five $XLF^{\Delta/\Delta}$ (443 metaphases), six $53BP1^{-/-}$ (377 metaphases), and seven $XLF^{\Delta/\Delta}53BP1^{-/-}$ mice (405 metaphases). In these analyses, average levels of chromosomal abnormalities were found in 7% of WT, 30% of $Ku70^{-/-}$, 10% of $XLF^{\Delta/\Delta}$, and 14% of of $53BP1^{-/-}$ fibroblasts. These relative levels of chromosomal abnormalities in the different backgrounds were consistent with results from other studies with different cell types (19, 23, 24). The level of genomic abnormalities in $XLF^{\Delta/\Delta}53BP1^{-/-}$ fibroblasts was 27%, much greater than that of either $XLF^{\Delta/\Delta}$ or $53BP1^{-/-}$ fibroblasts and similar to that of fibroblasts deficient for the Ku70 C-NHEJ factor (30%; Fig. 4). In all lines, chromosomal breaks were much more dominant than chromatid breaks (Fig. 4*A*), suggesting that most of the unrepaired DNA breaks occurred in G1 when C-NHEJ is the dominant joining pathway. We conclude that repair of general chromosomal breaks in the G1 cell-cycle phase in $XLF^{\Delta/\Delta}53BP1^{-/-}$ cells is much more impaired than what is observed in the absence of either factor alone, with impairment reaching those observed in the absence of C-NHEJ.

Discussion

XLF and ATM have functionally redundant activities in promoting C-NHEJ, as this process is severely impaired in the absence of both factors but not in the absence of either factor alone. On the basis of studies of chromosomal V(D)J recombination, the functionally redundant activities of ATM with XLF involve the ATM kinase activity. Correspondingly, H2AX shows a similar, but not totally identical, functional redundancy with XLF in V(D)J recombination. The latter two findings suggested that the functional redundancy of ATM with XLF might be mediated more broadly through ATM DSB response substrates, potentially involving their assembly into foci around DSBs to promote fully efficient C-NHEJ (3). The 53BP1 protein is another ATM substrate that participates in DSB response foci, but which has been found to have only a modest role in normal V(D)J recombination (11, 13). Our current studies demonstrate that 53BP1 also has a major functional redundancy with XLF in promoting the C-NHEJ step of V(D)J recombination. Thus, inactivation of both XLF and 53BP1 severely impairs lymphocyte development at the progenitor stage when V(D)J recombination occurs and also substantially impairs V(D)J recombination CE and SE joining in a fashion strikingly similar to that found in the context of combined XLF and H2AX deficiency (3). Combined deficiency for XLF and 53BP1 also results in substantially increased genomic instability in nonlymphoid cells, most likely indicating that these two factors may have functional redundancy in C-NHEJ more generally, although there are other possible explanations. We conclude that XLF has overlapping functions with multiple members of the ATM DSB response pathway (ATM, H2AX, and 53BP1) in promoting C-NHEJ during V(D)J recombination and likely in promoting C-NHEJ more generally.

A

Spontaneous genomic instability in tail fibroblasts

Genotype	Total metaphases	Abnormal metaphases		Chromosomal breaks	Chromatid breaks
	n	n	%	n	n
WT (1)	60	2	3.3	2	0
WT (2)	115	16	13.9	22	4
WT (3)	47	2	4.3	2	0
WT (4)	108	6	5.6	6	0
WT (5)	41	2	4.9	1	1
WT (6)	17	1	5.9	1	0
WT (7)	21	0	0.0	0	0
WT (8)	57	3	5.3	3	1
Total	**466**	**32**	**6.9**		
XLF (1)	86	9	10.5	9	2
XLF (2)	72	7	9.7	5	2
XLF (3)	84	11	13.1	24	6
XLF (4)	80	8	10.0	6	4
XLF (5)	121	8	6.6	10	2
Total	**443**	**43**	**9.7**		
53BP1 (1)	40	9	22.5	7	2
53BP1 (2)	103	14	13.6	19	3
53BP1 (3)	109	12	11.0	15	2
53BP1 (4)	42	5	11.9	7	1
53BP1 (5)	43	5	11.6	3	2
53BP1 (6)	40	6	15.0	8	1
Total	**377**	**51**	**13.5**		
XLF/53BP1 (1)	25	7	28.0	12	0
XLF/53BP1 (2)	59	15	25.4	20	3
XLF/53BP1 (3)	51	19	37.3	24	2
XLF/53BP1 (4)	46	16	34.8	21	1
XLF/53BP1 (5)	82	17	20.7	15	4
XLF/53BP1 (6)	69	16	23.2	22	1
XLF/53BP1 (7)	73	20	27.4	34	3
Total	**405**	**110**	**27.2**		
Ku70 (1)	97	32	33.0	44	8
Ku70 (2)	83	28	33.7	36	10
Ku70 (3)	107	26	24.3	34	6
Total	**287**	**86**	**30.0**		

B

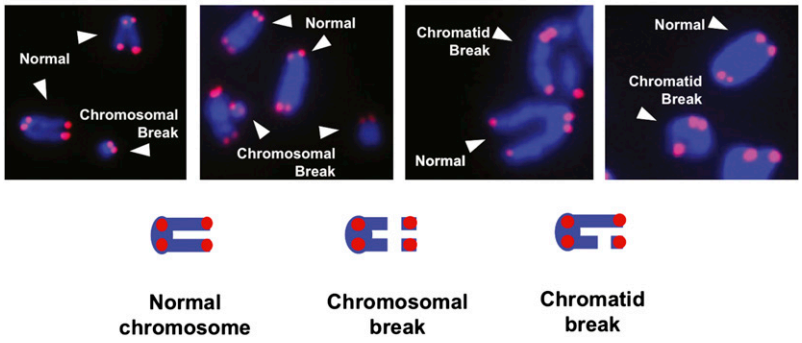

Fig. 4. Genomic instability in XLF/53BP1 double-deficient fibroblasts. (*A*) Telomere FISH analysis of abnormal metaphases in WT, $XLF^{\Delta/\Delta}$, $53BP1^{-/-}$, $XLF^{\Delta/\Delta}/53BP1^{-/-}$, and $Ku70^{-/-}$ fibroblasts. (*B*) Spontaneous cytogenetic abnormalities in fibroblasts. Examples of intact (normal) chromosomes and chromosomal (two *Left* panels) and chromatid (two *Right* panels) breaks. Red signal represents telomeres (Cy3); DNA is visualized with DAPI (blue).

However, the stable incorporation of 53BP1 into extended DSB response foci requires a process in which early events include γ-H2AX generation around DSBs via ATM phosphorylation. This process continues a cascade of events that include MDC-1 binding to γ-H2AX followed by recruitment of RNF8 by MDC1, leading to recruitment of RNF168, which then generates histone modifications leading to long-range 53BP1 accumulation in DSB response foci (25, 26). Our finding that ATM, H2AX, and 53BP1 all have functionally redundant roles with XLF in V(D)J recombination and C-NHEJ supports the notion that such redundant XLF functions may reflect those provided in the context of the general DSB response. In the context of XLF deficiency, ATM deficiency appears to more severely impair V(D)J joining than 53BP1 or H2AX deficiency alone. This finding could suggest additive effects of roles of downstream ATM factors in the same process and/or unique roles for individual DSB factors. In this context, H2AX and 53BP1 might have overlapping functions in DSB joining during ATM-dependent DSB complex formation that are different from their functions in end protection. Inactivation of additional ATM family members in the context of XLF deficiency should help elucidate unique or overlapping roles for 53BP1, H2AX, and other members of the pathway with XLF. Finally, as 53BP1 can be transiently recruited to DSBs independently of ATM or γ-H2AX (9), the possibility arises that it may serve a redundant function with XLF in that context.

As discussed previously for ATM or H2AX (3), functional redundancy for 53BP1 with XLF in C-NHEJ might be directly overlapping (e.g., influences on end-tethering and protection) and/or indirectly overlapping (e.g., influencing reaction kinetics versus influencing stability of repair complexes or checkpoints allowing their repair). In this regard, ATM mediates quite differential aspects of the DSB response. Through roles that include substrate phosphorylation, ATM promotes the physical joining of DNA ends, potentially by stabilizing them and protecting them from degradation (10). On the other hand, ATM can also activate nucleases, such as CtIP, that resect free ends (21). The balance between ATM end-stabilizing and resection activities may shift in different phases of the cell cycle to enhance DNA end protection in G1 and to promote C-NHEJ and enhance DNA end resection in S/G2 phase to promote HR (18). In this context, it is notable that XLF, as it does with

H2AX, has a functionally redundant role with 53BP1 in protecting unjoined CEs and SEs from being resected during V(D)J recombination. Notably, the degree of end-resection appears to be potentially more severe in cells doubly deficient in XLF and either H2AX or 53BP1 versus those deficient in H2AX and either Artemis or Lig4 (3, 21; this study), consistent with a potential role for XLF in end protection per se. On the other hand, the presence of XLF is not sufficient to prevent the increased ATM-dependent resection of unjoined CEs in the Artemis- or Lig4-deficient cells also deficient for H2AX (21). In this regard, XLF, in theory, might also contribute an overlapping function with H2AX and 53BP1 in end-protection indirectly by promoting efficient joining of ends and, thereby, preventing them from persisting as substrates for resection. Finally, we note that these two different types of proposed roles for XLF are not mutually exclusive.

The substantial general genomic instability that we observe in the context of combined XLF and 53BP1 deficiency could well reflect a general C-NHEJ deficiency. In this context, the growth retardation of $XLF^{\Delta/\Delta}53BP1^{-/-}$ mice, similar to that observed in the context of core C-NHEJ deficiencies, might reflect excessive unrepaired DNA DSBs leading to cell-cycle checkpoint activation and programmed cell death. It is notable that $XLF^{\Delta/\Delta}ATM^{-/-}$ and $XLF^{\Delta/\Delta}53BP1^{-/-}$ mice are viable whereas $XLF^{\Delta/\Delta}H2AX^{-/-}$ mice die embryonically (3). This finding may reflect ATM-independent functions for H2AX in S phase that are distinct from S-phase functions of 53BP1, which is consistent with findings that H2AX deficiency leads to a higher level of S-phase–associated chromosomal lesions (chromatid breaks) than ATM or 53BP1 deficiency that mainly leads to prereplicative lesions (chromosome breaks) (23). Alternatively, both ATM and 53BP1 are involved in checkpoint activation processes not provided by H2AX. Thus, although loss of either ATM or 53BP1 alone might substantially impair C-NHEJ, the cellular effects of this deficiency might be ameliorated by additional checkpoint defects. In this regard, deficiency for either p53 or ATM rescues embryonic lethality of Lig4 deficiency (27, 28). If this model is correct, one might predict a similar rescue of XRCC4 deficiency by 53BP1 deficiency.

Materials and Methods

Mice. $XLF^{+/\Delta}$, $53BP1^{+/-}$, and HL mice have been described previously (3, 11, 20). All HL mice were heterozygous for both IgH and IgL knock-in alleles (+/K).

Chromosomal V(D)J Recombination Assays. V(D)J recombination with an integrated substrate was carried out as described. Briefly, *v-abl*–transformed pro–B-cell lines were isolated from various mouse lines that harbored an Eμ-Bcl-2 transgene. The pro-B lines were infected with the pMX-Del-CJ or pMX-Del-SJ retroviral vector and assayed for V(D)J recombination as described. ATM inhibitor Ku55933 (EMD Biosciences; catalog no. 118500) was used at a final concentration of 15 μM as described.

Lymphocyte Development. Lymphocyte populations were analyzed by flow cytometry as described (3).

Generation of Primary Murine Tail Fibroblasts. Mouse tail skin was removed, cut into ~4-mm^2 pieces, and treated with 1.6 mg/mL collagenase II (Gibco) in DMEM supplemented with 10% (vol/vol) heat-inactivated FCS and antibiotics for 24 h [37 °C, 5% (vol/vol) CO_2 incubator]. After filtration through a 70-μm nylon cell strainer (BD Falcon), cells were washed in DMEM/10% (vol/vol) FCS and plated. Fibroblasts from the second or third passage were used for the telomere FISH assay. Because we obtained and used fibroblasts at the same passage number across individual mice, variability in fibroblast recovery limited the number of metaphases per mouse available for a given analysis.

Telomere FISH Assay. Fibroblasts were treated with 100 ng/mL colcemid (KaryoMAX Colcemid solution; Gibco) for 4 h. Then the cells were incubated in trypsin–PBS, washed with PBS, swollen in 75 mM KCl at 37 °C for 20 min, and fixed in methanol:acetic acid (3:1) for the metaphase analysis as described previously (19, 23). Telomeres were stained with a Cy3-labeled CCCTAACCCTAACCCTAA probe (PNA; Applied Biosystems), and DNA was visualized with DAPI. Images were acquired with an Eclipse microscope (Nikon). Chromosomal breaks were defined by loss of telomere signal from both sister chromatids, whereas chromatid breaks had no telomere signal at one of the two sister chromatids or a clear lack of DAPI signal in the middle of one chromatid.

ACKNOWLEDGMENTS. We thank Dr. B. Sleckman for providing $53BP1^{-/-}$ mice with a Bcl2 transgene. This work is supported by National Institutes of Health Grant AI076210 (to F.W.A.). D.R.W. is supported by National Institutes of Health Grant K08AI89972 and by an award from the American Association of Allergy Asthma and Immunology and CSL Behring and holds a Career Award for Medical Scientists from the Burroughs Wellcome Fund. F.W.A. is an investigator of the Howard Hughes Medical Institute. C.G. is a fellow of Cancer Research Institute.

1. Gostissa M, Alt FW, Chiarle R (2011) Mechanisms that promote and suppress chromosomal translocations in lymphocytes. *Annu Rev Immunol* 29:319–350.
2. Zhang Y, et al. (2010) The role of mechanistic factors in promoting chromosomal translocations found in lymphoid and other cancers. *Adv Immunol* 106:93–133.
3. Zha S, et al. (2011) ATM damage response and XLF repair factor are functionally redundant in joining DNA breaks. *Nature* 469:250–254.
4. Bassing CH, Alt FW (2004) The cellular response to general and programmed DNA double strand breaks. *DNA Repair (Amst)* 3:781–796.
5. Rooney S, Chaudhuri J, Alt FW (2004) The role of the non-homologous end-joining pathway in lymphocyte development. *Immunol Rev* 200:115–131.
6. Lee GS, Neiditch MB, Salus SS, Roth DB (2004) RAG proteins shepherd double-strand breaks to a specific pathway, suppressing error-prone repair, but RAG nicking initiates homologous recombination. *Cell* 117:171–184.
7. Deriano L, et al. (2011) The RAG2 C terminus suppresses genomic instability and lymphomagenesis. *Nature* 471:119–123.
8. Yan CT, et al. (2007) IgH class switching and translocations use a robust non-classical end-joining pathway. *Nature* 449:478–482.
9. Celeste A, et al. (2003) Histone H2AX phosphorylation is dispensable for the initial recognition of DNA breaks. *Nat Cell Biol* 5:675–679.
10. Bredemeyer AL, et al. (2006) ATM stabilizes DNA double-strand-break complexes during V(D)J recombination. *Nature* 442:466–470.
11. Manis JP, et al. (2004) 53BP1 links DNA damage-response pathways to immunoglobulin heavy chain class-switch recombination. *Nat Immunol* 5:481–487.
12. Yin B, et al. (2009) Histone H2AX stabilizes broken DNA strands to suppress chromosome breaks and translocations during V(D)J recombination. *J Exp Med* 206: 2625–2639.
13. Ward IM, et al. (2004) 53BP1 is required for class switch recombination. *J Cell Biol* 165: 459–464.
14. Reina-San-Martin B, Chen J, Nussenzweig A, Nussenzweig MC (2007) Enhanced intra-switch region recombination during immunoglobulin class switch recombination in 53BP1-/- B cells. *Eur J Immunol* 37:235–239.
15. Boboila C, et al. (2010) Alternative end-joining catalyzes robust IgH locus deletions and translocations in the combined absence of ligase 4 and Ku70. *Proc Natl Acad Sci USA* 107:3034–3039.
16. Difilippantonio S, et al. (2008) 53BP1 facilitates long-range DNA end-joining during V(D)J recombination. *Nature* 456:529–533.
17. Bothmer A, et al. (2010) 53BP1 regulates DNA resection and the choice between classical and alternative end joining during class switch recombination. *J Exp Med* 207: 855–865.
18. Bunting SF, et al. (2010) 53BP1 inhibits homologous recombination in Brca1-deficient cells by blocking resection of DNA breaks. *Cell* 141:243–254.
19. Zha S, Alt FW, Cheng HL, Brush JW, Li G (2007) Defective DNA repair and increased genomic instability in Cernunnos-XLF-deficient murine ES cells. *Proc Natl Acad Sci USA* 104:4518–4523.
20. Li G, et al. (2008) Lymphocyte-specific compensation for XLF/cernunnos end-joining functions in V(D)J recombination. *Mol Cell* 31:631–640.
21. Helmink BA, et al. (2011) H2AX prevents CtIP-mediated DNA end resection and aberrant repair in G1-phase lymphocytes. *Nature* 469:245–249.
22. Ward IM, Minn K, van Deursen J, Chen J (2003) p53 binding protein 53BP1 is required for DNA damage responses and tumor suppression in mice. *Mol Cell Biol* 23: 2556–2563.
23. Franco S, et al. (2006) H2AX prevents DNA breaks from progressing to chromosome breaks and translocations. *Mol Cell* 21:201–214.
24. Ferguson DO, et al. (2000) The nonhomologous end-joining pathway of DNA repair is required for genomic stability and the suppression of translocations. *Proc Natl Acad Sci USA* 97:6630–6633.
25. Stewart GS (2009) Solving the RIDDLE of 53BP1 recruitment to sites of damage. *Cell Cycle* 8:1532–1538.
26. Noon AT, Goodarzi AA (2011) 53BP1-mediated DNA double strand break repair: Insert bad pun here. *DNA Repair (Amst)* 10:1071–1076.
27. Lee Y, Barnes DE, Lindahl T, McKinnon PJ (2000) Defective neurogenesis resulting from DNA ligase IV deficiency requires Atm. *Genes Dev* 14:2576–2580.
28. Frank KM, et al. (2000) DNA ligase IV deficiency in mice leads to defective neurogenesis and embryonic lethality via the p53 pathway. *Mol Cell* 5:993–1002.